

This item is the archived peer-reviewed author-version of:

Synergism of the initial stage of removal of dielectric materials during electrical erosion processing in electrolytes

Reference:

Zaripov A.A., Khalilov Umedjon, Ashurov Kh. B.- Synergism of the initial stage of removal of dielectric materials during electrical erosion processing in electrolytes

Surface engineering and applied electrochemistry - ISSN 1934-8002 - 59:6(2023), p. 712-718

Full text (Publisher's DOI): <https://doi.org/10.3103/S1068375523060194>

To cite this reference: <https://hdl.handle.net/10067/2027540151162165141>

Synergism of the Initial Stage of Removal of Dielectric Materials during Electrical Erosion Processing in Electrolytes

A. A. Zaripov^{a,*}, U. B. Khalilov^{a,b}, and Kh. B. Ashurov^a

^a Institute of Ion Plasma and Laser Technologies, Academy of Sciences of the Republic of Uzbekistan, Tashkent, 100125 Uzbekistan

^b University of Antwerp, NANOLab Center for Advanced Research, PLASMANT Scientific Group, Antwerp, 2610 Belgium

Abstract—Ceramics and composites, many of whose physicochemical properties significantly exceed similar properties of metals and their alloys, are processed qualitatively mainly by the electroerosion method. Despite the existing works, the mechanism of the initial stage of the removal of materials has not yet been identified. For a comprehensive understanding of the mechanism of the removal of dielectrics, a new model is proposed based on the experimental results obtained on an improved electroerosion installation. It was revealed that the initial stage of the removal of a dielectric material consists of three successive stages that are associated with the synergistic effect on the process of the anionic group of electrolytes, plasma flare, and the cavitation shock. This makes it possible to better understand the mechanism of the removal of composite and ceramic materials, which should contribute to ensuring the machinability of those materials and their wide use in promising technologies.

Keywords: electroerosion treatment, material removal mechanism, material removal rate, synergetic effect, cavitation, bubbles, collapse, electrolytes, anionic group, plasma flame, pulse discharge

INTRODUCTION

Composite and ceramic materials are successfully used in aerospace engineering [1], on railway transport [2], in mechanical engineering [3], in missile components and hypersonic vehicles [4], in the civil infrastructure system [5], in biomedicine [6, 7], etc. Their widespread use is facilitated by the variety of physical and mechanical characteristics and chemical composition, which make it possible to create materials with pre-calculated properties [8–10]. Despite the advantages of composites and ceramics described above, their processing is fraught with great difficulties. In particular, machining, although it has a preference when processing metals [11], leads to unacceptable quality of parts made of ceramic and composite materials [12] and reduces long-term reliability [13]. Therefore, only nonmechanical methods, such as laser, ultrasonic, electrochemical, and electrical discharge, are allowed for processing [14]. Electroerosion treatment (EET) differs from other nonmechanical methods in its cost-effectiveness and ability to process composite materials with complex profiles [15]. When processing dielectrics, electrical discharge methods are used in combination with other methods, such as the auxiliary electrode method [16], electrochemical [17], ultrasonic [18], and laser processing [19, 20]. However, despite some advantages of these combined methods, the EET method using electrolytes is more practical and effective when processing ceramics and composites [21].

Although various removal models for ceramics and composites are known, the removal mechanism of EET using electrolytes is still a matter of debate. The scientific debate about processing mechanisms has led to several proposed models of the process. For example, Melk et al. [22], based on the processing of 3Y-TZP composite multiwalled carbon nanotubes, concluded that material removal occurs due to melting, evaporation, and cracking. However, the contribution of the appearance and existence of discharges, as well as the role of the physicochemical properties of electrolytes at all stages of processing, were not taken into account [23]. Yue et al. [24], through experiments and simulations, showed the capabilities of the thermal, mechanical, and chemical nature of CFRP removal. In [25], the effect of thermal stress on the material removal of carbon fiber reinforced silicon carbide was studied and it was determined that high cutting speed was associated with thermal stress. Additionally, Rajput et al. [26], based on the processing of quartz, glass, and ceramics, showed that the mechanism of material removal includes thermal erosion, chemical etching, and thermal cracking. Dutta et al. [27] determined the percentage contribution of voltage, pulse duration, and rotation frequency of the tool electrode (TE) into material removal rate (MRR). They argued that removal occurs precisely due to melting and evaporation. Klock et al. [28] found significant discrepancies when comparing measured processing temperatures to preexisting models. In addition, other components of material removal, such as the influence of pulsed discharges and the bubble layer near the cathode [29], are not taken into account in the works described above [24–26].

Despite the existence of a number of studies, the available results do not provide an opportunity to fully and comprehensively understand the nature of material removal. In this article, we will focus on the mechanism of the initial stage of dielectric removal during processing in electrolytes.

EXPERIMENTAL SETUP

For EET of dielectrics in electrolytes an improved electrical erosion device with a relaxation generator was developed [30], which is shown in Fig. 1. The installation consists of a tracking compensating system in the form of a floating head with a conical cathode and a damper holder. The sample, located on a damper holder, is pressed against the anode tip and placed inside a bath filled with NaOH or KOH or NaCl electrolyte.

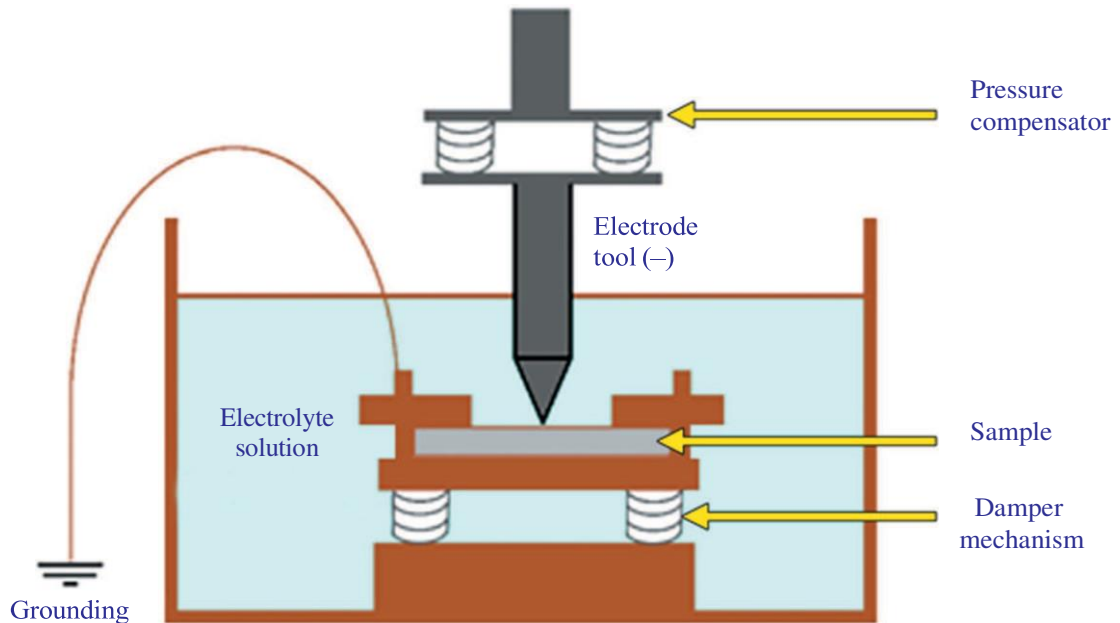


Fig. 1. Schematic illustration of an electroerosive device for removing dielectrics in electrolytes.

A potential difference is created between the electrolyte and the cathode. The output voltage of the unit can be adjusted in the range of 0–400 V, and the maximum current is up to 10 A. The objects of research are glass (as a composite [31, 32]) with the chemical composition of 68.4% SiO₂, 8.5% CaO, 9.4% Na₂O, 7.1% K₂O, 3.9% Al₂O₃, 2.7% B₂O₃, and Alumina Ceramics (Al₂O₃). The surface of the samples was examined using an NLCD-307B optical microscope.

RESULTS AND ITS DISCUSSION

Figure 2a shows a dielectric sample that has not been subjected to electrical discharge machining. After treatment in electrolyte, the edges of the holes are not ideal for the circle (see Fig. 2b), as in the case of heat treatment [33]. In particular, on the treated surface of the hole, sequences of chips and bulges are clearly visible, which are not a consequence of melting or heat treatment. Similarly, Paul et al. [34] determined that increasing electrolyte concentration leads to irregular circle and hole shapes.

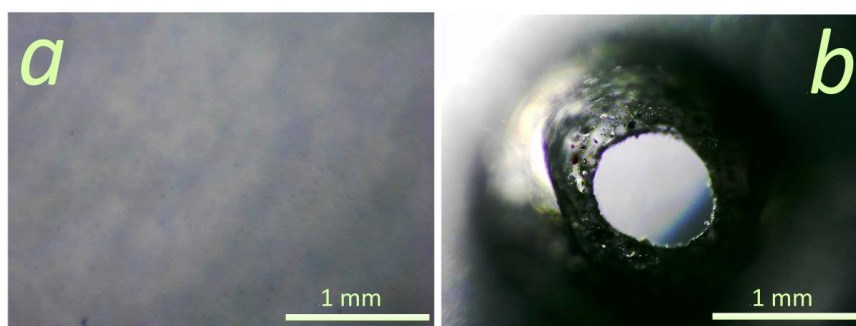


Fig. 2. Sample of a glass plate (a) before and (b) after electrical discharge machining in an electrolyte.

Yan et al. [35] also consider that a nonrotating cathode will result in an irregular hole shape. In general, a visual assessment of the pierced holes with a rotating cathode and the conclusions of the above-mentioned authors do not allow us to conclude that they are a consequence of heat treatment. However, such an assessment does not allow us to draw definitive conclusions.

A more universal assessment for all processing methods is to determine the material removal rate [36, 37]. The results showed that the MRR of electrical erosion in electrolytes depends on two important factors: electrical power and electrolyte type. In particular, the dependence of MRR on the input electrical power is shown in Fig. 3: at 36 W in 6% aqueous electrolytes NaOH, KOH, and NaCl, the material removal rates are 1.3, 1.35, and 0.11 mm³/s; at 70 W they are 4.5, 4.65, and 0.36 mm³/s, respectively. Obviously, the numerical values of MRR increase by more than three times and have a linear dependence on the supplied electrical power in the studied range of 35–75 W. The resulting linear dependence of MRR on the supplied electrical power is identical to the theoretical dependence for polyelectrolytes [38]. However, this linearity does not depend only on the input power but may be related to the physicochemical properties of the electrolyte. For example, Mohammad et al. [39] report that part of the discharge energy is absorbed by the workpiece due to conduction, while the rest is dissipated in the electrolyte due to convection and radiation. Wei et al. [40, 41] calculated that the share of power transferred to the part in discharge mode is only 29%. In this situation, Bilal et al. [42] consider that thermal cracking and spalling are the main driving force in dielectric EET. Rajput et al. [43] also prefer the material removal mechanism as a thermal model. Although the thermal model agrees well with existing simulation models, the difference between the calculated values [43] and experimentally observed [21, 44] is significant. In particular, depending on the material, the temperature in simulation models exceeds 3300 K, and in practical measurements using a thermocouple tungsten–iron and spectral analysis cathode, the temperature is 2300 ± 200 K [21, 44]. Moreover, the results of Slovetsky and Terentyev (where the cathode temperature does not exceed 1500 K) are generally consistent with the above conclusions [45]. In addition, the temperature of the electrolyte at a distance of 2 mm from the gas-discharge (or bubble) layer, even at high cathode temperatures, does not exceed the boiling point of water (100°C) [45–49]. In our case, the melting temperature of ceramic samples was higher than 3000 K [50, 51]. Therefore, we believe that the removal of material does not occur due to heat treatment. This means that the linear increase in MRR with increasing input electrical power is not associated with thermal effects but depends on other factors, for example, on the physicochemical properties (i.e., type or concentration) of the electrolyte. In particular, the dependences of MRR on capacity and electrolyte type are shown in Fig. 3.

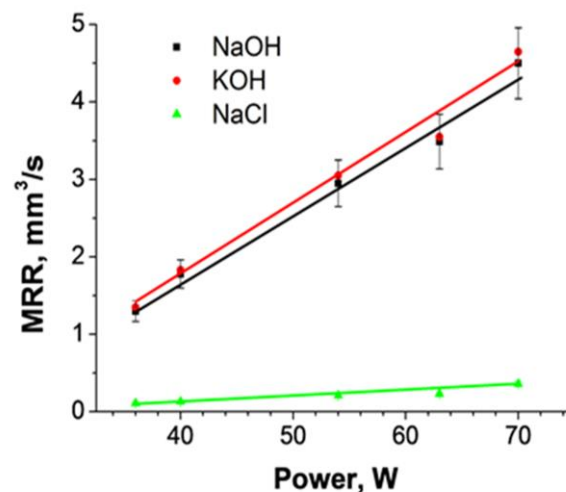


Fig. 3. Dependence of the glass plate removal rate on the supplied power in aqueous solutions of NaCl, NaOH, and KOH electrolytes

The results prove that samples in alkaline solutions are processed at approximately the same speed, and an order of magnitude greater than when processed in table salt. Namely: changing the anionic group with Cl⁻ on OH⁻ leads to an increase in MRR by an order of magnitude and an increase in the intensity of the appearance of hydrogen bubbles at the cathode [52]. Paul et al. [53] have also achieved significant increases in MRR using potassium and sodium hydroxides in semiconductor processing. In addition, although the dependence of MRR on electrolyte type is very strong, MRR is independent of electrolyte concentration in the studied range (5–27%). It is obvious that the processing process is associated not only with the physicochemical properties of the electrolyte but also with an external factor, for example, the frequency characteristics of the relaxation generator [54].

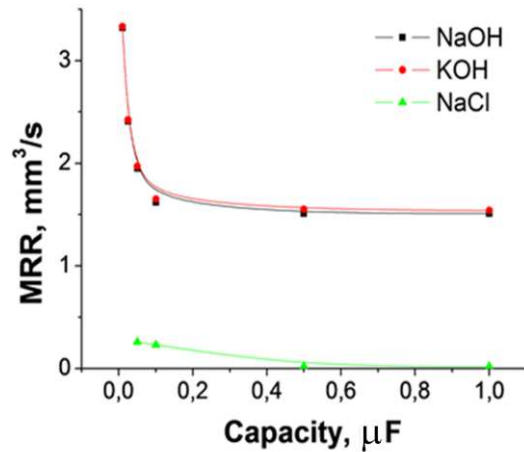


Fig. 4. Dependence of the glass plate removal rate on the capacitor capacity in aqueous solutions of NaCl, NaOH, and KOH electrolytes.

Figure 4 shows a graph of the dependence of MRR on the capacitor capacitance, which determines the frequency characteristics of the discharge in an RC generator. In particular, for aqueous solutions of NaOH, KOH, and NaCl at 1 \square F, the removal rates are 1.51, 1.54, and 0.022 mm³/s, while those at 0.01–0.05 \square F are 3.32, 3.33, and 0.36 mm³/s, respectively. The results show that, for smaller capacitor values, the MRR is higher than for relatively larger capacitors. Ali et al. [55] found that capacitor capacitance is the most important parameter for creating a conductive layer in a nonconductive ceramic. It is known that the capacitance of the capacitor is linearly related to the pulse duration (\square) in RC oscillators (that is, $\square = RC$). Dutta et al. [27], using the Taguchi method, determined that the effect of pulse duration on MRR is significant, that is, the share among other influencing factors exceeds 5%. Khan et al. [56] improved the surface quality due to discharge branching, which led to an increase in the pulse frequency. Yang et al. [57] also showed that increasing the frequency of the discharge pulse expands the treated surface area and produces less thermal energy. Obviously, reducing the capacitance of the capacitor or the pulse duration leads to improved and faster processing of the dielectric.

Based on the analysis of the results described above and existing literature data, the mechanism of dielectric removal in its initial stage can be divided into three stages (see Fig. 5a). At the initial stage (see Fig. 5a, I), the usual process of electrolysis occurs, which is associated with the possibility of the formation of point defects with different types of conductivity in electrolytes [58]. The current-voltage characteristic (volt-ampere characteristic) in this region has a linear dependence (see Fig. 5b, I).

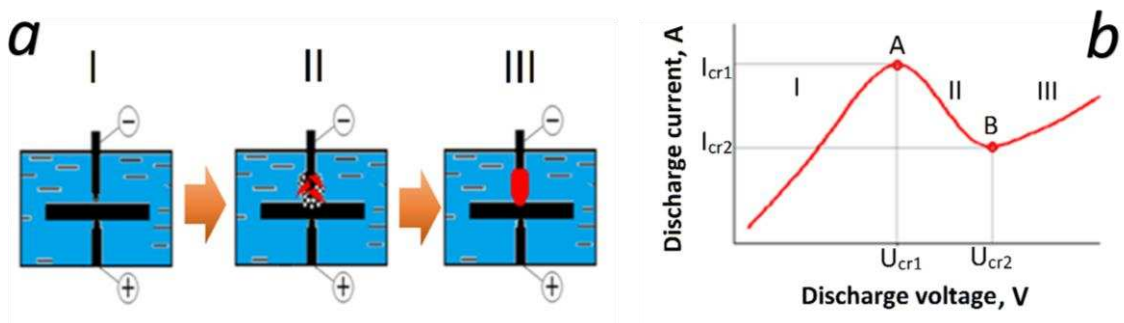


Fig. 5. (a) Schematic representation of the initial stage of the EET of dielectrics process, consisting of three stages; (b) volt-ampere characteristics of electrolytes for three stages of the initial stage of the EET process.

This process continues until a threshold (critical) or ionic (anionic) current occurs (see Fig. 5b II, A) at which initial bubbles and subsequent discharges appear. This value strongly depends on the physicochemical properties, that is, on the type of electrolyte [21]. In particular, the critical current and voltage at a concentration of 6% for NaCl, NaOH, and KOH electrolytes are 50 V and 1.8 A, 25 V and 2 A, and 25 V and 1.9 A, respectively. In the case of NaCl, the increased critical voltage is associated with the electrolyte resistance between the electrodes, which is twice as high as in the case of NaOH and KOH. The results also showed that

the general character of the current-voltage characteristic is identical at all stages for other electrolyte concentrations.

The beginning of the second stage is characterized by the formation of bubbles on the surface of the cathode (see Fig. 5a, II). The reason for the appearance of bubbles and increased gas formation is associated with an increase in the local temperature of the electrolyte near the cathode (for example, the average gas temperature in experiments is 900 K [45]) due to a further increase in input voltage. An increase in the concentration of bubbles near the cathode leads to a gradual insulation of the cathode surface. Clusters of bubbles and accompanying initial discharges cannot exist separately. The formation of a large number of small bubbles on the cathode enhances these discharges [59]. Due to the appearance of an insulating bubble layer in the electrolyte, the total electric current consists of conduction current and displacement current [60]. Displacement currents arise in the insulating bubble layer in a nonstationary mode when an alternating electric field is applied to this medium [61]. At the boundary of the electrolyte and the bubble layer (which insulates part of the cathode), the ion (anion) current and the displacement currents are compensated. Consequently, the ionic current flows only through the remaining uninsulated part of the cathode. Although the bias currents increase sensitively, the total (total) current decreases due to the strong drop in ion current. In particular, the total current and voltage at point B (see Fig. 5b II) for electrolytes NaCl, NaOH, and KOH at a concentration of 6% are 110 V and 1.3 A, 65 V and 0.6 A, and 65 V and 0.6 A, respectively. The decrease in the critical current at the cathode is associated with an increase in the resistance of the electrolyte and the insulating bubble layer between the electrodes. At the end of the second stage, stable vapor-gas layers (average thickness 0.5 mm) appear near the cathode due to the maximum accumulation of bubbles. Consequently, high-frequency discharges begin to slip through these layers.

The final stage is characterized by cavitation phenomena [23], as well as a plasma luminous torch (with a characteristic lifetime of 5 ms [62]), existing due to the increasing frequency of high-frequency discharges near the cathode (see Fig. 5a, III). At the beginning of the third stage, the bubbles of the vapor-gas layer begin to collapse due to the balancing of internal and external pressure due to an increase in local temperature, which is a derivative of the applied voltage. Therefore, the collapse of bubbles, called cavitation [63], leads to the occurrence of a large cavitation shock, which is approximately 10^{10} MPa [23]. Therefore, Kuo et al. [64] used cavitation to improve MRR through specially created bubbles. It is due to cavitation that the surface area of the insulating vapor-gas layer decreases, which leads to a subsequent moderate increase in the discharge current on the current-voltage characteristic (see Fig. 5b, III). At the same time, the Coulomb forces of a luminous plasma plume of ionized gas affect the surface roughness of a dielectric consisting of dipoles. Another party involved in the processes are the anionic groups of electrolytes (Cl^- OH^-). These groups serve to change atomic bonds due to their attachment to the surface atoms of the sample [52]. At the same time, the anionic group and the plasma effect, mutually complementing each other, lead to a weakening of atomic bonds on the surface of dielectric samples, and, consequently, the receipt shock breaks the bond. The breaking of atomic bonds due to the synergistic effect of the above three factors can be considered the beginning of the EET process.

CONCLUSIONS

In this paper, we proposed a new model for the removal mechanism of dielectric materials based on the analysis of previously existing traditional models. Material removal was experimentally studied using an advanced EET machine, which resulted in a significant increase in the material removal rate (MRR).

In particular, we determined that the initial stage of removal of dielectric materials consists of three successive stages: first, the process of conventional electrolysis (I) occurs, then a bubble layer is formed at the cathode (II) and high-frequency discharges become more frequent, followed by the appearance of a plasma torch near the cathode and cavitation (III). It has been established that the mechanism of the initial stage of material removal is associated with the synergistic effect of the interaction of the anionic group of electrolytes, the burning plasma torch, and cavitation impact. In general, the results show that the proposed synergetic model covers all the main processes of the mechanism of the initial stage of material removal and to a significantly greater extent than traditional thermal models.

Basically, the measurements and their analysis allow us to better understand the process of EET of dielectrics in order to increase MRR, which implies expanding the possibility of using composite and ceramic materials in promising industries.

REFERENCES

1. Soutis, C., Aerospace engineering requirements in building with composites, in *Polymer Composites in the Aerospace Industry*, Irving, Ph. and Soutis, C., Eds., Woodhead Publishing, 2020, p. 3.
2. Robinson, M., Matsika, E. and Peng, Q., Application of composites in rail vehicles, in *Reference Module in Materials Science and Materials Engineering*, 2016, Elsevier, p. 1.
3. Mavhungu, S.T., Akinlabi, E.T., Onitiri, M.A., and Varachia, F.M., Aluminum matrix composites for industrial use: Advances and trends, *Procedia Manuf.*, 2017, vol. 7, p. 178.
4. Binner, J., Porter, M., Baker, B., Zou, J., et al., Selection, processing, properties and applications of ultra-high temperature ceramic matrix composites, UHTC-MCs—a review, *Int. Mater. Rev.*, 2020, vol. 65, no. 7, p. 389.
5. Ganga Rao, H., Infrastructure applications of fiber-reinforced polymer composites, in *Applied Plastics Engineering Handbook*, William Andrew Publishing, 2017, p. 675.
6. Mann, G.S., Singh, L.P., Kumar, P., and Singh, S., Green composites: A review of processing technologies and recent applications, *J. Thermoplast. Comp. Mater.*, 2020, vol. 33, no. 8, p. 1145.
7. Boccardi, E., Ciraldo, F.E., and Boccaccini, A.R., Bio-active glass-ceramic scaffolds: Processing and properties, *MRS Bull.*, 2017, vol. 42, no. 3, p. 226.
8. Ralbag, N., Mann-Lahav, M., Davydova, E.S., Ash, U., et al., Composite materials with combined electronic and ionic properties, *Matter*, 2019, vol. 1, no. 4, p. 959.
9. Li, Zh., Zhang, X., Cheng, H., Liu, J., et al., Confined synthesis of 2D nanostructured materials toward electrocatalysis, *Adv. Energy Mater.*, 2020, vol. 10, no. 11, p. 1900486.
10. Li, N., Huang, S., Zhang, G., Qin, R., et al., Progress in additive manufacturing on new materials: A review, *J. Mater. Sci. Technol.*, 2019, vol. 35, no. 2, p. 242.
11. Costa, C., Ferreira, L.P., Sá, J.C., Silva, F.J., et al., Implementation of 5S methodology in a metalworking company, in *DAAAM International Scientific Book*, Branko Katalinic, Ed., Vienna: DAAAM International Editor, 2018, p. 1.
12. Heidary, H., Karimi, N.Z., and Minak, G., Investigation on delamination and flexural properties in drilling of carbon nanotube/polymer composites, *Comp. Struct.*, 2018, vol. 201, p. 112.
13. Xu, J., Li, Ch., Mi, S., An, Q., et al., Study of drilling-induced defects for CFRP composites using new criteria, *Comp. Struct.*, 2018, vol. 201, p. 1076.
14. Bilal, A., Jahan, M.P., Talamona, D. and Perveen, A., Electro-discharge machining of ceramics: A review, *Micromachines*, 2018, vol. 10, no. 1, p. 10.
15. Rayat, M.S., Gill, S.S., Singh, R. and Sharma, L., Fabrication and machining of ceramic composites: A review on current scenario, *Mater. Manuf. Proc.*, 2017, vol. 32, no. 13, p. 1451.
16. Mohri, N., Fukuzawa, Y., Tani, T., Saito, N., et al., Assisting electrode method for machining insulating ceramics, *CIRP Annals*, 1996, vol. 45, no. 1, p. 201.
17. Abitov, A.R., Electrophysical and chemical processing of shaped surfaces in silicon workpieces, *Extended Abstract of Cand. Sci. (Phys.–Math.) Dissertation*, Tula, 2011.
18. Leon, A.V., Zvyadintseva, S.Yu., Chirkov, E.A., Shkodin, A.S., et al., Classification of the main areas of research on hybrid processes, *Mekhanika XXI veku*, 2019, no. 18, p. 196.
19. Al-Ahmari, A.M.A., Rasheed, M.S., Mohammed, M.K., and Saleh, T., A hybrid machining process combining micro-EDM and laser beam machining of nickel–titanium-based shape memory alloy, *Mater. Manuf. Proc.*, 2016, vol. 31, no. 4, p. 447.
20. Li, L., Diver, C., Atkinson, J., Giedl-Wagner, R., et al., Sequential laser and EDM micro-drilling for next generation fuel injection nozzle manufacture, *CIRP Annals*, 2006, vol. 55, no. 1, p. 179.
21. Abdurkarimov, E.T., Mirkarimov, A.S., and Zaripov A.A., Electroerosion treatment of dielectric materials, *Surf. Eng. Appl. Electrochem.*, 2007, vol. 43, no. 2, p. 77.
22. Melk, L., Antti, M.L., and Anglada, M., Material removal mechanisms by EDM of zirconia reinforced MWCNT nanocomposites, *Ceram. Int.*, 2016, vol. 42, no. 5, p. 5792.
23. Zaripov, A.A. and Ashurov, Kh.B., Phenomenological mechanism of the effect of cavitation on EEO glass, *Elektron. Obrab. Mater.*, 2014, vol. 50, no. 2, p. 105.
24. Yue, X., Yang, X., Tian, J., He, Z., et al., Thermal, mechanical and chemical material removal mechanism of carbon fiber reinforced polymers in electrical discharge machining, *Int. J. Machine Tools Manuf.*, 2018, vol. 133, p. 4.
25. Yue, X., Li, Q., and Yang, X., Influence of thermal stress on material removal of Cf/SiC composite in EDM, *Ceram. Int.*, 2020, vol. 46, no. 6, p. 7998.
26. Rajput, V., Goud, M., and Suri, N.M., Study on effective process parameters: Toward the better comprehension of EDCM process, *Int. J. Mod. Manuf. Technol.*, 2019, vol. 11, no. 2, p. 105.
27. Dutta, H., Debnath, K., and Sarma, D.K., A study of material removal and surface characteristics in micro-electrical discharge machining of carbon fiber reinforced plastics, *Polym. Compos.*, 2019, vol. 40, no. 10, p. 4033.
28. Klocke, F., Mohammadnejad, M., Zeis, M. and Klink, A., Investigation on the variability of existing models for

- simulation of local temperature field during a single discharge for electrical discharge machining (EDM), *Procedia CIRP*, 2018, vol. 68, p. 260.
29. Zaripov, A.A. and Ashurov, Kh.B., Contributions of various factors to the process of electric pulse processing, *Uzb. Fiz. Zh.*, 2016, vol. 18, no. 3, p. 214.
 30. Zaripov, A.A., Processes during electrical discharge machining of dielectrics, *Extended Abstract of Doctoral Dissertation*, Tashkent: Inst. Ion-Plasma Laser Tech- nol. Acad. Sci. Repub. Uzb., 2019.
 31. Pahlevani, F. and Sahajwalla, V., Effect of glass aggre- gates and coupling agent on the mechanical behaviour of polymeric glass composite, *J. Cleaner Prod.*, 2019, vol. 227, p. 119.
 32. Thomason, J.L., Glass fibre sizing: A review, *Compos. Part A: Appl. Sci. Manuf.*, 2019, vol. 127, p. 105619.
 33. Furutani, K. and Maeda, H., Machining a glass rod with a lathe-type electro-chemical discharge machine, *J. Micromech. Microeng.*, 2008, vol. 18, no. 6, p. 065006.
 34. Paul, L. and Hiremath, S.S., Improvement in machin- ing rate with mixed electrolyte in ECDM process, *Pro- cedia Technol.*, 2016, vol. 25, p. 1250.
 35. Yan, B.H., Wang, A.C., Huang, C.Y. and Huang, F.Y., Study of precision micro-holes in borosilicate glass us- ing micro EDM combined with micro ultrasonic vibration machining, *Int. J. Machine Tools Manuf.*, 2002, vol. 42, no. 10, p. 1105.
 36. Bobbili, R., Madhu, V., and Gogia, A.K., Effect of wire-EDM machining parameters on surface roughness and material removal rate of high strength armor steel, *Mater. Manuf. Proc.*, 2013, vol. 28, no. 4, p. 364.
 37. Mohammadi, A., Tehrani, A.F., Emanian, E., and Karimi, D., Statistical analysis of wire electrical dis- charge turning on material removal rate, *J. Mater. Pro- ces. Technol.*, 2008, vol. 205, nos. 1–3, p. 283.
 38. Ashurov, Kh.B. and Zaripov, A.A., Experimental study and model description of a pulsed corona discharge near a solid body placed in a strong electrolyte, *Dokl. Akad. Nauk Uzb.*, 2013, no. 1, p. 26.
 39. Mohammad, Y.A., Maleque, M.A., Banu, A., Sabur, A., et al., Micro electro discharge machining of non-con- ductive ceramic, *Mater. Sci. Forum*, 2018, vol. 911, p. 20.
 40. Wei, C., Xu, K., Ni, J., Brzezinski, A.J., et al., A finite element based model for ECDM in discharge regime, *Int. J. Adv. Manuf. Technol.*, 2011, vol. 54, p. 987.
 41. Wei, C., Hu, D., Xu, K., and Ni, J., Electro chemical discharge dressing of metal bond micro grinding tools, *Int. J. Machine Tools Manuf.*, 2011, vol. 51, p. 165.
 42. Bilal, A., Perveen, A., Talamona, D., and Jahan, M.P., Understanding material removal mechanism and ef- fects of machining parameters during EDM of zirco- nia-toughened alumina ceramic, *Micromachines*, 2021, vol. 12, no. 1, p. 67.
 43. Rajput, V., Goud, M., and Suri, N.M., Finite element modeling based material removal analysis of non-con- ductive materials in ECDM using adaptive tool feed system, *Int. J. Mod. Manuf. Technol.*, 2020, vol. 12, no. 1, p. 164.
 44. Kirko, D.L., Oscillatory processes in the plasma of the discharge in electrolyte in a magnetic field, *Tech. Phys.*, 2015, vol. 60, no. 4, p. 505.
 45. Slovetskii, D.I. and Terent'ev, S.D., Electric discharge in electrolytes as a source of nonequilibrium plasma at atmospheric pressure, *Khim. Vys. Energii*, 2003, vol. 37, no. 5, p. 355.
 46. Fascio, V., Wiithrich, R., Viquerat, D., and Langen H., 3D micro structuring of glass using ECDM, in *Proc. Int. Symposium on Micromechatronics and Human Sci- ence*, 1999, p. 179.
 47. Fascio, V., Langen, H.H., Bleuler, H., and Comminel- lis, C., Investigations of the SACE, *Electrochem. Com- mun.*, 2003, vol. 5, p. 203.
 48. Basak, I. and Ghosh, A., Mechanism of spark genera- tion during electrochemical discharge machining: A theoretical model and experimental verification, *J. Ma- ter. Process. Technol.*, 1996, vol. 62, nos. 1–3, p. 46.
 49. Fascio, V., Wuthrich, R. and Bleuler, H., SACE in the light of electrochemistry, *Electrochim. Acta*, 2004, vol. 49, p. 3997.
 50. Gu, M., Huang, C., Xiao, S. and Liu, H., Improve- ments in mechanical properties of TiB₂ ceramics tool materials by the dispersion of Al₂O₃ particles, *Mater. Sci. Eng.: A*, 2008, vol. 486, nos. 1–2, p. 167.
 51. Schneider, S.J. and McDaniel, C.L., Effect of environ- ment upon the melting point of Al₂O₃, *J. Res. Nat. Bureau Standards. Sect. A, Phys. Chem.*, 1967, vol. 71, no. 4, p. 317.
 52. Jalali, M., Maillard, P., and Wüthrich, R., Toward a better understanding of glass gravity-feed micro-hole drilling with electrochemical discharges, *J. Micromech. Microeng.*, 2009, vol. 19, no. 4, p. 045001.
 53. Paul, L. and Hiremath, S.S., Improvement in machining rate with mixed electrolyte in ECDM process, *Procedia*

Technol., 2016, vol. 25, p. 1250.

54. Zaripov, A.A. and Ashurov, Kh.B., Electrical discharge machining of nonconductive materials, *Surf. Eng. Appl. Electrochem.*, 2011, vol. 47, no. 3, p. 197.
55. Mohamed A.R., Asfana B. and Mohammad Y.A., Investigation of recast layer of non-conductive ceramic due to micro-EDM, *Adv. Mater. Res.*, 2014, vol. 845, p. 857.
56. Han, M.S., Min, B.K., and Lee, S.J., Improvement of surface integrity of electro-chemical discharge machining process using powder-mixed electrolyte, *J. Mater. Process. Technol.*, 2007, vol. 191, nos. 1–3, p. 224.
57. Yang, C.T., Song, S.L., Yan, B.H. and Huang, F.Y., Improving machining performance of wire electro-chemical discharge machining by adding SiC abrasive to electrolyte, *Int. J. Machine Tools Manuf.*, 2006, vol. 46, no. 15, p. 2044.
58. Macdonald, D.D., The history of the point defect model for the passive state: a brief review of film growth aspects, *Electrochim. Acta*, 2011, vol. 56, no. 4, p. 1761.
59. Descoedres, A., Characterization of electrical discharge machining plasmas, Thèse no. 3542, Lausanne, EPFL, 2006.
60. Siegel, D.M., *Innovation in Maxwell's Electro-Magnetic Theory: Molecular Vortices, Displacement Current, and Light*, Cambridge University Press, 2003.
61. Ivchenkov, G., Displacement currents in metals, dielectrics and vacuum. <http://new-idea.kulichki.net/pubfiles/190712004817.pdf>.
62. Abdurkarimov, E.T., Mirkarimov, A.M., Zaripov, A.A., Study of electrical discharge in an aqueous electrolyte solution, *Uzb. Fiz. Zh.*, 2003, vol. 5, no. 1, p. 52.
63. Brennen, C.E., *Cavitation and Bubble Dynamics*, Cambridge University Press, 2014.
64. Kuo, K.Y., Wu, K.L., Yang, C.K. and Yan, B.H., Wire electrochemical discharge machining (WECDM) of quartz glass with titrated electrolyte flow, *Int. J. Machine Tools Manuf.*, 2013, vol. 72, p. 50.